hasil-Analysis of a Mathematical Model of the Interaction between PIP3, AKT, and FOXO3a in Acute Myeloid Leukemia

by Yudi Ari Adi

Submission date: 20-Apr-2022 08:53AM (UTC+0700)
Submission ID: 1815027047
File name: J4.2020-IJAM_50_1_26.pdf (4.42M)
Word count: 8058
Character count: 34798

Analysis of a Mathematical Model of the Interaction between PIP3, AKT, and FOXO3a in Acute Myeloid Leukemia

Yudi Ari Adi, Lina Aryati, Fajar Adi-Kusumo, and Mardiah Suci Hardianti

***Abstract*—The model of interaction between PIP3, AKT, and FOXO3a in the PI3K/AKT signaling pathways in Acute Myeloid Leukemia (AML) is described and analyzed in this paper. We assume that the biochemical reaction in this pathway follows Hill's equation and consider the case that the mechanism of protein dephosphorylation does not work properly. Then, we analyze the model using the stability theory of differential equations to determine the parameters that play an important role in AML disease. Firstly, we discuss the existence of steady states and their stability. Furthermore, numerical simulations are given to support the analytical results of the model. Sensitivity index is also analyzed to identify parameters which have a significant influence on AML disease and should be targeted by intervention strategies. Our results show how targeted therapy can be performed on the PI3K/AKT pathway for the treatment of AML.**

***Index Terms*—PI3K/AKT pathway, Mathematical model, Stability, Sensitivity analysis.**

I. Introduction

ACUTE Myeloid Leukemia (AML) is the most common hematological malignancies in hematopoietic system characterized by deregulated proliferation of immature myeloid cells [1]. Commonly, there is deregulation of PI3K/AKT pathways in AML patients, which is about 50 to 80 % of AML patients undergoing phosphorylation of AKT on Thr 308 and Ser 473 [2], [3], [4]. The AKT phosphorylation is associated with significantly elevated levels of phosphorylated FOXO3a in AML blast cells which later suppresing its normal function in induction apoptosis and cell cycle regulations [5], [6], [7]. Normally, FOXO3a transcriptionally activates several genes as the target. The FOXO3a binds to an administrator of apoptosis-inducing genes, such as Bim, FasL, and TRAIL, and a promoter of cell cycle inhibitors, such as p27 and p21. The FOXO3a also activates autophagy genes Gabarapl1, ATG12, etc. [8], [9]. The studies in [7], [10], [9] have shown that phosphorylation of FOXO3a is associated with increased proliferation, low overall survival, and an adverse prognosis factor in AML patient.

Manuscript received July 9, 2019; revised January 13, 2020. This work was supported in part by the Ministry of Research and Higher Education (Kemenristek DIKTI) of Indonesia.

Yudi Ari Adi is with the Department of Mathematics, Faculty of Applied Science and Technology, Universitas Ahmad Dahlan, Yogyakarta 55191, Indonesia email:yudi.adi@math.uad.ac.id.

Lina Aryati and Fajar Adi-Kusumo are with the Department of Mathematics, Faculty of Mathematics and Natural Sciences, Universitas Gadjah Mada, Yogyakarta 55281, Indonesia.

Mardiah S. Hardianti is with the Department of Internal Medicine, Faculty of Medicine, Public Health, and Nursing, Universitas Gadjah Mada, Yogyakarta 55281, Indonesia.

Mathematical models of hematopoiesis provide a framework for study leukemia genesis and treatment strategies. Several mathematical models have been constructed to explain various aspects of leukemia diseases. These models have been applied to evaluate the existing therapies and to design combination therapies or to suggest novel therapies. A brief review of some mathematical models for leukemia has been conducted by Clapp & Lay [11]. Recently, Besse et al. [12] have studied a model of interaction between cancer cells and immune systems in a Chronic Myeloid Leukemia. For mathematical modeling in biopathways, several models in recent decades have been published by many authors such as in [13], [14], [15], [16]. However, in our knowledge of those model, there is no modeling that studies dynamics of AML cells at functional levels. In recent decades, the PI3K/AKT pathway has received considerable attentions as a potential therapeutic target in malignancy diseases including AML.

Previously, Adi et al. [17] proposed a mathematical model describing an interaction of protein in PI3K/AKT pathways. The model was motivated by some recent studies that some promising new agents are currently in advanced development to treat AML. The treatment was divided into three categories based on the mechanisms of their actions: cytotoxic agents, small-molecule inhibitors, and targeted therapies [3], [18], [19]. Recent preclinical or clinical developments have shown that many patients with AML have considered being treated with a small molecule inhibitor that targets molecules in PI3K/AKT pathways [1], [18]. The modeling results suggested that PIP3, phosphorylated AKT protein, and phosphorylated FOXO3a are potentially targeted to AML therapy. However, the most influential parameters that used as a measure on the sustainability of AML disease could not be determined analytically.

In a disease management point of view, it is necessary to identify the range of parameter values so that the disease either can be healed or persists. Mathematically, the identification process can be done through a stability analysis of the equilibrium point of the model. Motivated by that notion, in this paper, we propose a new model that describes interactions between proteins in PI3K/AKT pathways. A mathematical analysis of the model is carried out by first simplifying the model developed. The simplification is done by adding assumptions on the model so that it is sufficiently accessible to conduct the mathematical analysis. The results of these analyses can be used as an alternative reference in AML treatment strategy.

The organization of this paper is as follows. In the next section, we will present our mathematical model. In Section 3, we discuss properties of the solutions and equilibria of

the model. In section 4, we analyze existences and local stabilities of the equilibria. In section 5, some numerical simulations are given to support the theoretical results. Next, in section 6, we do a sensitivity analysis to describe how local changes in parameter values affect system behaviors. Finally, conclusion and discussion are provided in Section 7.

II. Model Formulation

In [17], Adi et al constructed a mathematical model that describes the dynamics of interaction between some molecules in PI3K/AKT pathways. The model was given as a system of ODEs in five equations, describing the dynamics of phosphatidylinositol trisphosphate (PIP3), AKT protein kinases, phosphorylated AKT protein kinase, forkhead transcription factor-3a (FOXO3a), and phosphorylated FOXO3a (FOXO3ap). In this paper, we improved the model [17] by adding an assumption that FOXO3a as a transcriptional regulator always exists in a certain amount within the nucleus [8]. Under this assumption, we found that the phosphorylation of FOXO3a has a disruption that also follow Hill's Equation. The disruption is represented by $\frac{k_4 x_3 x_4^2 \Lambda}{K_4^3+x_4^3}$, where the parameter Λ is residual of FOXO3a in the nucleus. We note that Hill's function is commonly used for sigmoidal binding behavior as a characteristic of cooperative binding mechanisms [20]. This is convenient to estimate the number of ligand molecules that are required to bind the receptor in order to produce a functional effect [21].

We also consider that in AML, the mechanism of protein dephosphorylation does not proceed normally, due to a decrease in a level of phosphatase or the presence of phosphatase deletions, i.e. PTEN and PP2A [5], [10]. According to this fact, we assume that the dephosphorylation of proteins does not occur. Also, the phosphorylation processes in the activation of AKT occur relatively faster than the degradation processes [22]. This condition leads us to assume that the degradation rate of AKT can be neglected. Therefore, the mathematical model is given in the following system of ODEs:

$$\begin{cases} \frac{dx_1}{dt} = k_0 + bx_5 - d_1 x_1 \\ \frac{dx_2}{dt} = a_2 - \frac{k_2 x_1 x_2^2}{K_2^2+x_2^2} \\ \frac{dx_3}{dt} = \frac{k_2 x_1 x_2^2}{K_2^2+x_2^2} - d_3 x_3 \\ \frac{dx_4}{dt} = (x_4 - \Lambda)\left((p - mx_4) - \frac{k_4 x_3 x_4^2}{K_4^3+x_4^3}\right) \\ \frac{dx_5}{dt} = \frac{k_4 x_3 (x_4-\Lambda) x_4^2}{K_4^3+x_4^3} - d_5 x_5. \end{cases} \quad (1)$$

together with the initial conditions:

$$x_1(0) \geq 0, x_2(0) \geq 0, x_3(0) \geq 0, x_4(0) \geq \Lambda, x_5(0) \geq 0, \quad (2)$$

where $x_1, x_2, x_3, x_4,$ and x_5 are the phosphatidylinositol trisphosphate (PIP3), AKT protein kinases, phosphorylated AKT protein kinase, forkhead transcription factor-3a (FOXO3a), and phosphorylated FOXO3a (FOXO3ap), respectively. Parameters $d_1, d_3,$ and d_5 represent the degradation rates of PIP3, AKT protein kinase, phosphorylated AKT protein kinase, and phosphorylated FOXO3a, respectively. Parameters $k_0, a_2,$ and p are the production rate of PIP3, AKT, and FOXO3a, respectively. Parameters $k_2,$ and k_4 are the phosphorylattion rates of AKT and FOXO3ap, respectively. Parameter m is the degradation rate of FOXO3a by protein 14-3-3, whereas parameters K_2 and K_4 represent the Michaelis constants of AKT phosphorylation and FOXO3ap, respectively.

In the next section, we will discuss the solution properties of the model (1) which include the positivity, boundedness, and uniqueness of the solution.

III. Properties of Solution

In order for the system (1) to have biological meaningful, it is necessary to show that system solutions with positive initial conditions will always be positive and bounded. This is shown in the following lemma.

Lemma 3.1 (*Positivity*). *The set* $\Omega = \{(x_1, x_2, x_3, x_4, x_5)\} \in R_+^5 \cup \{0\} : x_4 \geq \Lambda\}$ *is positive invariant for System* (1) *with initial conditions* (2).

Proof. Let $\mathbf{x} = (x_1, x_2, x_3, x_4, x_5)$ and $\mathbf{n}_i, i = 1, 2, 3, 4, 5$ is a normal vector to the segment $x_1 = 0, x_2 = 0, x_3 = 0, x_4 = \Lambda,$ and $x_5 = 0$ inward the domain Ω. We have $\mathbf{n}_1 = (1, 0, 0, 0, 0), \mathbf{n}_2 = (0, 1, 0, 0, 0), \mathbf{n}_3 = (0, 0, 1, 0, 0), \mathbf{n}_4 = (0, 0, 0, 1, 0),$ and $\mathbf{n}_5 = (0, 0, 0, 0, 1)$. Then, we calculate the dotproduct of normal vector $\mathbf{n}_i$ with vector field $\dot{\mathbf{x}}$. As we see, $\mathbf{n}_1 \cdot \dot{\mathbf{x}} = 1 \cdot \dot{\mathbf{x}}_1 + 0 \cdot \dot{\mathbf{x}}_2 + 0 \cdot \dot{\mathbf{x}}_3 + 0 \cdot \dot{\mathbf{x}}_4 + 0 \cdot \dot{\mathbf{x}}_5 = k_0 + bx_5 \geq 0$, Since the value of dotproduct is not negative, this means that the vector field will be in the same direction as a normal vector, i.e. inside the domain Ω. Analogous calculations can be applies along other parts of boundaries they are all not negative. So, it can be concluded that the solution of system (1) together with initial conditions (2) exist for all $t \geq 0$ and $x_i(t) \in \Omega$. Therefore, it is proven that Ω is positive invariant.

Lemma 3.2 (*Boundedness*). *Let* $x_1(t), x_2(t), x_3(t), x_4(t),$ *and* $x_5(t)$ *are solution of system* (1) *There exist* $M > 0$, *such that* $\lim_{t\to\infty}$ *sup* $x_i(t) \leq M$, *for all* $t \in [0, T]$.

Proof. We must proof that for all $t \in [0, T]$, $x_1(t), x_2(t), x_3(t), x_4(t),$ and $x_5(t)$ will be bounded. We note that all of the parameter values used in the system (1) are positive.

From the fourth equation of system (1), we get

$$\begin{aligned} \frac{dx_4}{dt} &= (x_4 - \Lambda)\left((p - mx_4) - \frac{k_4 x_3 x_4^2}{K_4^3 + x_4^3}\right) \\ &\leq x_4\left((p - mx_4) - \frac{k_4 x_3 x_4^2}{K_4^3 + x_4^3}\right) \\ &\leq x_4(p - mx_4). \end{aligned}$$

Hence, we consider $\dot{u} = u(p - mu)$, which a solution $u(t) = \frac{u(0)\frac{p}{m}}{(\frac{p}{m} - u(0))e^{-pt} + u(0)}$, where $\lim_{t\to\infty}$ sup $u(t) = \frac{p}{m}$. We know that $\dot{x}_4(t) \leq \dot{u}(t)$, then by the comparison theorem [23],it implies that $\lim_{t\to\infty}$ sup $x_4(t) \leq \lim_{t\to\infty}$ sup $u(t) = \frac{p}{m} = M_1$.

Similarly, from the first and third equation of system (1) it follows that $\lim_{t\to\infty}$ sup $x_1(t) \leq \frac{k_0 mq + bp^2}{mqd_1} = M_1$, and $\lim_{t\to\infty}$ sup $x_3(t) \leq \frac{k_2 k_0 mq + k_2 bp^2}{mqd_1 d_3} = M_3$.

Now, from the fourth and fith equation of system (1), we get

$$\begin{aligned} \frac{dx_4}{dt} + \frac{dx_5}{dt} &= (x_4 - \Lambda)\left((p - mx_4) - d_5 x_5\right) \\ &\leq x_4\left((p - mx_4) - d_5 x_5\right) \\ &\leq \frac{p}{m}\left((p - mx_4) - d_5 x_5\right) \\ &\leq \frac{p^2}{m} - q\left(x_4 + x_5\right). \end{aligned}$$

where $q = min\{p, d_5\}$.

Therefore, $x_4(t)+x_5(t) \le \frac{p^2}{mq}+(x_4(0)+x_5(0)-\frac{p^2}{mq})e^{-qt}$, and $\lim_{t\to\infty}$ sup $(x_4(t)+x_5(t)) \le \frac{p^2}{mq} = M_5$. Thus, $x_4(t)+x_5(t)$ is bounded, so $x_5(t)$ is also bounded.

Similarly, from the second and third equation of system (1), we get

$$\frac{dx_2}{dt} + \frac{dx_3}{dt} = a_2 - d_3x_3 \le a_2,$$

this we have $x_2(t)-x_2(0)+x_3(t)-x_3(0) \le a_2t$ or $x_2(t) \le x_2(0)+x_3(0)+a_2t \le x_2(0)+x_3(0)+a_2T = M_2$.

Therefore, choose $M = \max\{M_1, M_2, M_3, M_4, M_5\}$, so that $x_i(t) \le M, i = 1, 2..5$, for all $t \in [0, T]$. This completes the proof.

Theorem 3.1 (*Existence and uniqueness*). *Let $\Omega > 0$. If the initial conditions of system (1) satisfy $x_1(0) > 0, x_2(0) > 0, x_3(0) > 0, x_4(0) > \Lambda, x_5(0) > 0$, then for all $t \in R, x_1(t), x_2(t), x_3(t), x_4(t), x_5(t)$ will exist in Ω.*

Proof. In system (1), we have

$$\mathbf{f(x)} = \begin{bmatrix} k_0 + bx_5 - d_1x_1 \\ a_2 - \frac{k_2x_1x_2^2}{K_2^2+x_2^2} \\ \frac{k_2x_1x_2^2}{K_2^2+x_2^2} - d_3x_3 \\ (x_4-\Lambda)\left((p-mx_4) - \frac{k_4x_3x_4^2}{K_4^3+x_4^3}\right) \\ \frac{k_4x_3(x_4-\Lambda)x_4^2}{K_4^3+x_4^3} - d_5x_5. \end{bmatrix}.$$

Since $\mathbf{f} \in C^1(R^5)$, thus $\mathbf{f}$ is locally Lipschitz in R^5, so that by Lemma 3.1, Lemma 3.2, and Fundamental existence and uniqueness theorem [23], we know that the solution of system (1) is exist and unique in Ω. This completes the proof.

Next, by simple calculation we have that system (1) has the AML-free equilibrium point

$$E_0 = \left(\frac{k_0}{d_1}, \frac{K_2\sqrt{a_2d_1}}{\sqrt{k_0k_2-a_2d_1}}, \frac{a_2}{d_3}, \Lambda, 0\right) \tag{3}$$

and the others equilibria

$$E_{1i}^* = (x_{1i}^*, x_{2i}^*, x_{3i}^*, x_{4i}^*, x_{5i}^*), \tag{4}$$

where

$$\begin{aligned} x_{1i}^* &= \tfrac{k_0}{d_1} + \tfrac{bk_4a_2x_{4i}^{*2}(x_{4i}^*-\Lambda)}{d_1d_3d_5\left(K_4^3+x_{4i}^{*3}\right)}, \\ x_{2i}^* &= \tfrac{K_2\sqrt{a_2d_1d_3d_5\left(K_4^3+x_{4i}^{*3}\right)}}{\sqrt{(k_0k_2-a_2d_1)d_3d_5\left(K_4^3+x_{4i}^{*3}\right)+bk_2k_4a_2x_{4i}^{*2}\left(x_{4i}^*-\Lambda\right)}}, \\ x_{3i}^* &= \tfrac{a_2}{d_3}, \\ x_{5i}^* &= \tfrac{k_4a_2x_{4i}^{*2}(x_{4i}^*-\Lambda)}{d_3d_5\left(K_4^3+x_{4i}^{*3}\right)} \end{aligned} \tag{5}$$

and $x_{4i}^*, i = 1, 2, 3, 4$ are positive solutions of the following equation:

$$x_4^4 + c_3x_4^3 + c_2x_4^2 + c_1x_4 + c_0 = 0, \tag{6}$$

with

$$c_3 = -\frac{p}{m}, \quad c_2 = \frac{a_2k_4}{md_3}, \quad c_1 = K_4^3, \quad c_0 = -\frac{pK_4^3}{m}. \tag{7}$$

IV. Existence and Local Stability of Equilibria

In this section, we deal with the existence and local stability of the equilibria. We note that the condition $k_0k_2 - a_2d_1 > 0$ guaranteed that the AML-free equilibrium point E_0 always exists.

A. The Existence of Equilibria

For the existence of the equilibriua $E_{1i}^*, i = 1, 2, 3, 4$, the solutions of (6) must be real and positive. The solutions of equation (6) are

$$\begin{aligned} x_{41}^* &= -\tfrac{c_3}{4} + \tfrac{1}{2}(S+D), \\ x_{42}^* &= -\tfrac{c_3}{4} + \tfrac{1}{2}(S-D), \\ x_{43}^* &= -\tfrac{c_3}{4} - \tfrac{1}{2}(S-F), \\ x_{44}^* &= -\tfrac{c_3}{4} - \tfrac{1}{2}(S+F). \end{aligned} \tag{8}$$

where

$$S = \sqrt{\frac{c_3^2}{4} - c_2 + u_1}, \tag{9}$$

$$D = \begin{cases} \sqrt{\frac{3c_3^2}{4} - S^2 - 2c_2 + \frac{1}{4S}(4c_2c_3 - 8c_1 - c_3^2)}, \text{if} S \ne 0 \\ \sqrt{\frac{3c_3^2}{4} - 2c_2 + 2\sqrt{u_1^2 - 4c_0}}, \quad \text{if} S = 0 \end{cases} \tag{10}$$

$$F = \begin{cases} \sqrt{\frac{3c_3^2}{4} - S^2 - 2c_2 - \frac{1}{4S}(4c_2c_3 - 8c_1 - c_3^2)}, \text{if} S \ne 0 \\ \sqrt{\frac{3c_3^2}{4} - 2c_2 - 2\sqrt{u_1^2 - 4c_0}}, \quad \text{if} S = 0 \end{cases} \tag{11}$$

with u_1 is a real root of cubic equation

$$u^3 - c_2u^2 + (c_1c_3 - 4c_0)u + (4c_0c_2 - c_1^2 - c_0c_3^2) = 0. \tag{12}$$

See [24], [25] for more detail about the cubic and quartic equation.

According to Descartes Rule of Sign, we can find that the equation (6) must have one or three positive real roots. We thus have the following results for the existence of the equilibria $E_{1i}^*, i = 1, 2, 3, 4$.

Theorem 4.1 *If $S = 0, k_0k_2 - a_2d_1 > 0$, and $x_{4i}^* > \Lambda, i = 1, ..., 4$, the following results hold:*

(i). *The system (1) has equilibrium point E_{11}^* whenever $16a_2k_4mp - 5d_3p^3 + 256m^3d_3K_4^3 \ge 0$ and $3d_3p^2 - 8a_2mk_4 \le 0$.*

(ii). *The equilibrium point E_{12}^* does not exist.*

(iii). *The system (1) has equilibrium point E_{13}^* whenever $16a_2k_4mp - 5d_3p^3 + 256m^3d_3K_4^3 \le 0$ and $3d_3p^2 - 8a_2mk_4 \ge 0$.*

(iv). *The system (1) has equilibrium point E_{14}^* whenever $16a_2k_4mp - 5d_3p^3 + 256m^3d_3K_4^3 \le 0$ and $d_3p^2 - 4a_2mk_4 \ge 0$.*

Proof. To prove the existence of the equilibria $E_{1i}^*, i = 1, ..., 4$ we use the existence $x_{4i}^*, i = 1, ..., 4$ in equation (6) which should be real and positive. From equation (9), $S = 0$ implies $u_1 = \frac{4ma_2k_4 - d_3p^2}{4d_3m^2}$. Clearly $-\frac{c_3}{4} = \frac{p}{4m}$ is real and positive, so x_{4i}^* in (8) is real and positive when D is real. After some simple calculations, we found that $x_{41}^* = -\frac{c_3}{4} + \frac{1}{2}(S+D)$ with $S = 0$ is real and positive when $16a_2k_4mp - 5d_3p^3 + 256m^3d_3K_4^3 \ge 0$ and $3d_3p^2 - 8a_2mk_4 \le 0$. The conditions of x_{4i}^* real and positive implies that the equilibrium point E_{11}^* exist. For conditions (ii), (iii), and (iv), the proofs are similar.

Theorem 4.2 *Let $A = \frac{p^2}{2m^2} - c_2 - u_1, B = 4c_2c_3 - 8c_1 - c_3^3, S = \sqrt{\frac{c_3^2}{4} - c_2 + u_1}, k_0k_2 - a_2d_1 > 0$, and $x_{4i}^* > \Lambda, i = 1, ..., 4$. If $S > 0$ then $u_1 > \frac{4a_2k_4m - d_3p^2}{4d_3m^2}$ and the following results hold:*

(i). *The equilibrium point E_{11}^* exist, whenever $A + \frac{B}{4S} \ge 0$.*

(ii). *The equilibrium point E_{12}^* exist, whenever$A + \frac{B}{4S} \ge 0$ and $B - \left(8u_1 + \frac{4p}{m}S\right)S < 0$.*

(iii). *The equilibrium point* E_{13}^* *exist, whenever* $A - \frac{B}{4S} \geq 0$ *and* $S - \frac{p}{2m} < \sqrt{A - \frac{B}{4S}}$.

(iv). *The equilibrium point* E_{14} *exist, whenever* $A - \frac{B}{4S} \geq 0$ *and* $\frac{p}{2m} - S > \sqrt{A - \frac{B}{4S}}$.

Proof. Using a procedure similar to the proof of Theorem 4.1, the existence of equilibriua E_{1i}^*, $i = 1, ..., 4$ for $S > 0$ also be done using the existence x_{4i}^*, $i = 1, ..., 4$ in equation (8) wich should be real and positive. From equation (9) $S > 0$ implies $u_1 > \frac{4a_2k_4m - d_3p^2}{4d_3m^2}$. To show that $x_{41}^* = \frac{p}{4m} + \frac{1}{2}(S + D)$ is real and positive, it is sufficient to prove that D is real. Finally, it is found that E_{11}^* exists, whenever $A + \frac{B}{4S} \geq 0$. The proof for (ii), (iii), and (iv) are similar.

B. *The Stability of equilibria*

In this subsection, we analyze the local stability of the equilibria by analyzing the eigenvalues of the Jacobian matrices of the system (1). The stability determined by the signs of real part of eigenvalues of the Jacobian matrix at a given equilibrium point. The Jacobian matrix for system (1) is given by

$$\begin{bmatrix} -d_1 & 0 & 0 & 0 & b \\ -\frac{k_2x_2^2}{K_2^2+x_2^2} & -\frac{2K_2^2k_2x_1x_2}{(K_2^2+x_2^2)^2} & 0 & 0 & 0 \\ \frac{k_2x_2^2}{K_2^2+x_2^2} & \frac{2K_2^2k_2x_1x_2}{(K_2^2+x_2^2)^2} & -d_3 & 0 & 0 \\ 0 & 0 & -\frac{k_4x_4^2(x_4-\Lambda)}{(K_4^3+x_4^3)} & a_{44} & 0 \\ 0 & 0 & \frac{k_4x_4^2(x_4-\Lambda)}{(K_4^3+x_4^3)} & a_{54} & -d_5 \end{bmatrix},$$

where

$$a_{44} = m\Lambda - \frac{(x_4-\Lambda)}{(K_4^3+x_4^3)^2}\left(2k_4x_3K_4^3x_4 - k_4x_3x_4^4\right) + p - 2mx_4 - \frac{k_4x_3x_4^2}{K_4^3+x_4^3},$$

and

$$a_{54} = \frac{\left(K_4^3+x_4^3\right)\left(k_4x_3x_4^2 + 2k_4x_3x_4\left(x_4-\Lambda\right)\right)}{\left(K_4^3+x_4^3\right)} \frac{-1}{\left(K_4^3+x_4^3\right)^2}\left(3k_4x_3x_4^4\left(x_4-\Lambda\right)\right).$$

For the local stability of AML-free equilibrium point E_0, we define the threshold value

$$\Gamma = \frac{p}{m\Lambda + \frac{k_4a_2\Lambda^2}{d_3\left(K_4^3+\Lambda^3\right)}}. \tag{13}$$

Then we have the following theorem.

Theorem 4.3 *The AML-free equilibrium point* E_0 *is locally asymptotically stable if* Γ *and unstable if* $\Gamma > 1$.

Proof. The eigenvalues of the Jacobian matrix of system (1) at equilibrium point $E_0 = \left(\frac{k_0}{d_1}, \frac{K_2\sqrt{a_2d_1}}{\sqrt{k_0k_2-a_2d_1}}, \frac{a_2}{d_3}, \Lambda, 0\right)$ are $\lambda_1 = -d_1$, $\lambda_2 = -\frac{2\sqrt{a_2d_1}\sqrt{(k_0k_2-a_2d_1)^3}}{k_0k_2K_2d_1}$, $\lambda_3 = -d_3, \lambda_4 = -d_5$, and $\lambda_5 = p - m\Lambda - \frac{k_4a_2\Lambda^2}{d_3\left(K_4^3+\Lambda^3\right)}$. We have four eigenvalues that always strictly negative. The fifth one, given by negative. The equilibrium point E_0 is locally asymptotically stable if $\lambda_5 = p - m\Lambda - \frac{k_4a_2\Lambda^2}{d_3\left(K_4^3+\Lambda^3\right)}$ negative, i.e. $p < m\Lambda + \frac{k_4a_2\Lambda^2}{d_3\left(K_4^3+\Lambda^3\right)}$ or $\frac{p}{m\Lambda+\frac{k_4a_2\Lambda^2}{d_3\left(K_4^3+\Lambda^3\right)}} < 1$. Thus the AML-free equilibrium point E_0 is locally asymptotically stable if $\Gamma < 1$ and unstable if $\Gamma > 1$. The proof is complete.

Next, we will find out the conditions for which the equilibria E_{1i}^*, $i = 1, 2, 3, 4$ are locally asymptotically stable. We define

$$\begin{aligned} Q &= \frac{a_2d_1d_3d_5\left(K_4^3+x_{4i}^{*3}\right)}{k_0d_3d_5\left(K_4^3+x_{4i}^{*3}\right)+bk_4a_2x_{4i}^{*2}(x_{4i}^*-\Lambda)}, \\ M &= \frac{2a_2\left(d_3d_5\left(K_4^3+x_{4i}^{*3}\right)(k_0k_2-a_2d_1)+bk_4a_2x_{4i}^{*2}(x_{4i}^*-\Lambda)\right)}{k_0k_2d_3d_5\left(K_4^3+x_{4i}^{*3}\right)+bk_4a_2x_{4i}^{*2}(x_{4i}^*-\Lambda)}, \\ C &= p - 2mx_{4i}^* + m\Lambda - \frac{(x_{4i}^*-\Lambda)\left(2k_4a_2K_4^3x_{4i}^*-k_4a_2x_{4i}^{*2}\right)}{d_3\left(K_4^3+x_{4i}^{*3}\right)^2} \\ &\quad - \frac{k_4a_2x_{4i}^{*2}}{d_3\left(K_4^3+x_{4i}^{*3}\right)}, \\ N &= \frac{k_4a_2x_{4i}^{*2}\Lambda+k_4a_2K_4^3x_{4i}^*(3x_{4i}^*-2\Lambda)}{d_3\left(K_4^3+x_{4i}^{*3}\right)^2}, \\ H &= \frac{k_4x_{4i}^{*2}(x_{4i}^*-\Lambda)}{\left(K_4^3+x_{4i}^{*3}\right)}, \\ \alpha_1 &= d_1 + d_3 + d_5 + M - C, \\ \alpha_2 &= d_3d_5 - (d_3+d_5)C + (M+d_1)(d_3+d_5-C) + d_1M, \\ \alpha_3 &= (M+d_1)(d_3d_5-(d_3+d_5)C) - d_3d_5C \\ &\quad + d_1M(d_3+d_5-C) - bQH \\ \alpha_4 &= d_1M(d_3d_5-(d_3+d_5)C) - (M+d_1)d_3d_5C \\ &\quad + b(C+N)QH, \\ \alpha_5 &= -d_1d_3d_5MC. \end{aligned} \tag{14}$$

Then, we find that the characteristic equation of system (1) corresponding to the equilibrium points $E_{1i}^* = (x_{1i}^*, x_{2i}^*, x_{3i}^*, x_{4i}^*, x_{5i}^*)$ is given by

$$\lambda^5 + \alpha_1\lambda^4 + \alpha_2\lambda^3 + \alpha_3\lambda^2 + \alpha_4\lambda + \alpha_5 = 0. \tag{15}$$

From the Routh-Hurwitz criterion, E_{1i}^*, $i = 1, 2, 3, 4$ are locally asymptotically stable if and only if $\alpha_1 > 0, \quad \alpha_3 > 0, \quad \alpha_5 > 0, \quad \Delta_2 > 0$,and $\Delta_4 > 0$, where $\Delta_2 = \alpha_1\alpha_2 - \alpha_3$, and $\Delta_4 = \alpha_1\alpha_2\alpha_3\alpha_4 + 2\alpha_1\alpha_4\alpha_5 - \alpha_1\alpha_2^2\alpha_5 - \alpha_1^2\alpha_4^2 - \alpha_3^2\alpha_4 - \alpha_5^2 + \alpha_2\alpha_3\alpha_5 > 0$.

It is obvious that $\alpha_1 > 0, \alpha_5 > 0$, and $\alpha_1\alpha_2 - \alpha_3 > 0$ if $C < 0$, that is

$$p - 2mx_{4i}^* + m\Lambda - \frac{(x_{4i}^*-\Lambda)\left(2k_4a_2K_4^3x_{4i}^*-k_4a_2x_{4i}^{*2}\right)}{d_3\left(K_4^3+x_{4i}^{*3}\right)^2} - \frac{k_4a_2x_{4i}^{*2}}{d_3\left(K_4^3+x_{4i}^{*3}\right)} < 0. \tag{16}$$

The other term of the Routh-Hurwitz condition can be verified by the numerical values of the parameter set as in Table I.

We summarize the above result in the Theorem 4.4 below.

Theorem 4.4 *The equilibrium points* $E_{1i}^*, i = 1, 2, 3, 4$ *is locally asymptotically stable if* $C < 0, \quad \alpha_3 > 0$, *and* $\Delta_4 > 0$.

In the next section we will give some numerical simulation to illustrate the theoretical results for several cases.

V. Simulation Results

In this section, we present some numerical simulations to demonstrate the theoretical results obtained in the previous section. The parameter values used in the system which given in Table I was obtained from Adi et al [17].

Case (i), AML-free quilibrium point. In this case, we take the parameter values $k_0 = 0.01, b = 0.0083, d_1 = 0.033, a_2 = 0.09, d_3 = 0.09, \Lambda = 0.2, p = 0.2, m = 0.28, k_2 = 1, K_2 = 0.1, k_4 = 0.04, K_4 = 0.1, d_5 = 0.125$.

With these values, the condition of Theorem 4.3 is satisfied. We have $\Gamma = 0.85551 < 1$ and the

TABLE I
PARAMETER VALUES AND KINETIC RATES BEING USED.

Parameter	Unit	Value
k_0	$\mu M min^{-1}$	0.01 – 0.1
b	min^{-1}	0.0083
d_1	min^{-1}	0.001 – 0.01
a_2	$\mu M min^{-1}$	0.036 – 0.108
k_2	min^{-1}	1 – 20
d_3	min^{-1}	0.0008 – 0.1
p	min^{-1}	0.002 – 0.5
m	$\mu M^{-1} min^{-1}$	0.004 – 0.28
k_4	min^{-1}	0 – 0.33
d_5	min^{-1}	0.033 – 0.125
K_2	μM	0.1
K_4	μM	0.1 – 1

system (1) has AML-free equilibrium point $E_0 = (0.30303, 0.064998, 1.000, 0.2, 0)$ which is locally aymptotically stable (see Fig.1).

Case (ii), The equilibria E^*_{1i}, $i = 1, 2, 3, 4$. In this case, we take the parameter values $k_0 = 0.01, b = 0.0083$, $d_1 = 0.02, a_2 = 0.09, d_3 = 0.09, \Lambda = 0.2, p = 0.33, m = 0.22, k_2 = 2, K_2 = 0.1, k_4 = 0.1, K_4 = 0.2, d_5 = 0.125$.

With these values, the equation (6) has one real root that satisfies the condition of Theorem 4.2(i), that is, $u_1 = -0.07024, \frac{4a_2k_4m-d_3p^2}{4d_3m^2} = -0.10795$, so we have $u_1 > \frac{4a_2k_4m-d_3p^2}{4d_3m^2}, A + \frac{B}{4S} = 1.4921 \geq 0$. The system (1) has one equilibrium point $E^*_{11} = (0.7689, 0.024931, 1.0000, 1.082867, 0.64816)$. In this case, the conditions of Theorem 4.4 are satisfied, that is, $C = -0,120816 < 0$, $\alpha_3 = 0,0080883 > 0$, and $\Delta_4 = 5,927949 \times 10^{-8} > 0$, so E^*_{11} is locally asymptotically stable (see Fig.2).

Next, we set the parameter values $k_0 = 0.01$, $b = 0.0083, d_1 = 0.033, a_2 = 0.09, d_3 = 0.09$, $\Lambda = 0.2$, $p = 0.36, m = 0.25, k_2 = 2$, $K_2 = 0.1, k_4 = 0.12$, $K_4 = 0.2, d_5 = 0.125$. With these parameter values, the equation (6) have three real r[43]s that satisfies the condition of existence E^*_{1i} in Theorem 4.2(i), 4.2(ii), and 4.2(iii), that is,$u_1 = 0.13706 > \frac{4a_2k_4-d_3p^2}{4d_3m^2} = -0.0384, A + \frac{B}{4S} = 0.51355 > 0, A - \frac{B}{4S} = 0.32593 > 0, B - \left(8u_1 + \frac{4p}{m}S\right)S = -1.31275 < 0, S - \frac{p}{2m} = -0.30112 < \sqrt{A - \frac{B}{4S}} = 0.5709$. The system (1) has three possible equilibria,

$$E^*_{11} = (0.49055, 0.03178, 1.0000, 0.92775, 0.74556),$$

$$E^*_{12} = (0.30991, 0.04122, 1.0000, 0.21113, 0.02735),$$

$$E^*_{13} = (0.42222, 0.03459, 1.0000, 0.43601, 0.4739).$$

We find that E^*_{11} and E^*_{12} are meet the condition of Theorer[44].4. Thus, E^*_{11} and E^*_{12} is locally asymptotically stable (see Fig.3 and Fig.4). In this case, E^*_{13} is unstable. According to the root of equation (15) we find that E^*_{13} is a sa[42]e point.

In the following Figs.1-4, we denote figure (a), (b), (c), and (d) as the dynamic between the FOXO3ap and PIP3, FOXO3ap and AKT, FOXO3ap and AKTp, and the dy[5]mic between FOXO3ap and FOXO3a, respectively. Fig.1 shows that the AML-free equilibrium point E_0 is locally asymptotically stable. We can see that all trajectories which starting

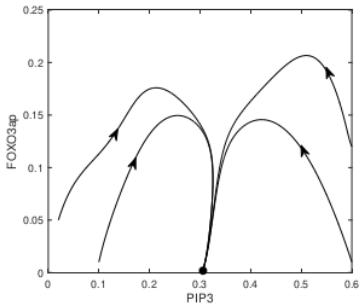

(a)

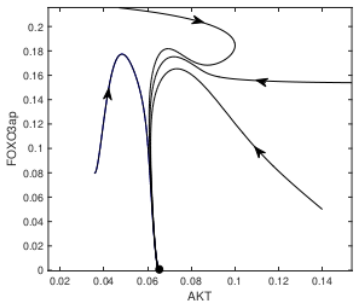

(b)

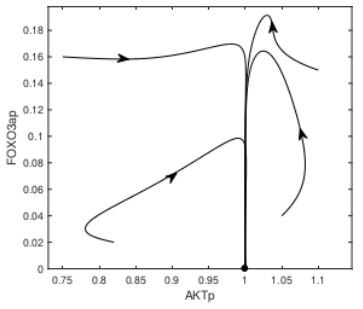

(c)

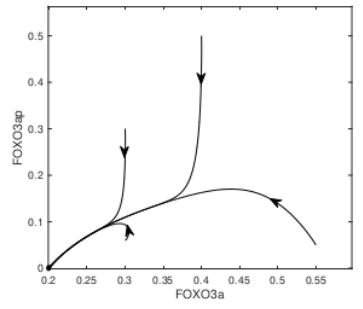

(d)

Fig. 1. The phase portrait projection confirms that the AML-free equilibrium point $E_0 = (0.30303, 0.064998, 1.000, 0.2, 0)$ is locally asymptotically stable.

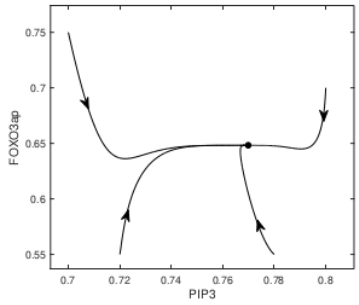

(a)

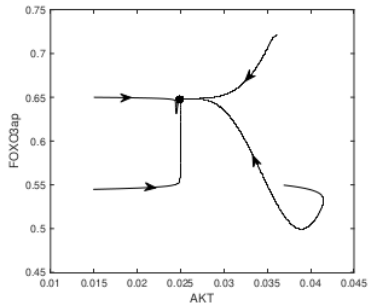

(b)

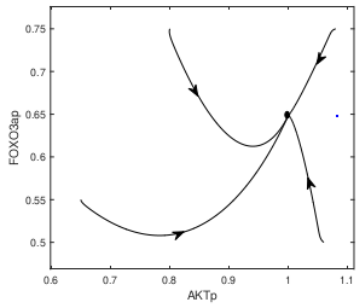

(c)

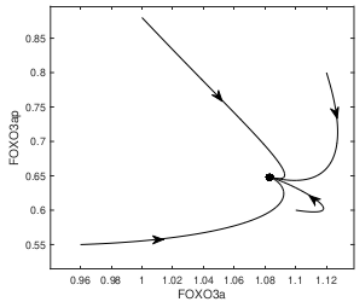

(d)

Fig. 2. The phase portrait projection confirms that the equilibrium point $E_{11}^{*} = (0.768986, 0.024931, 1.0000, 1.082867, 0.64816)$ is locally asyptotically stable.

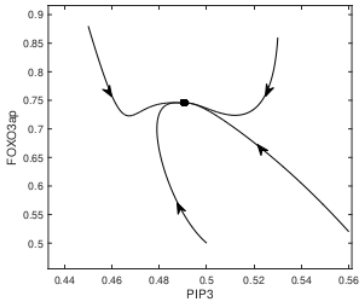

(a)

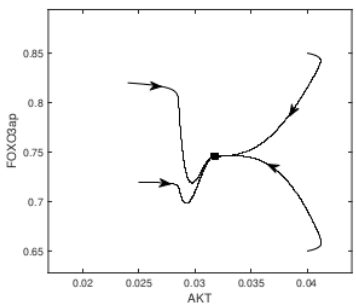

(b)

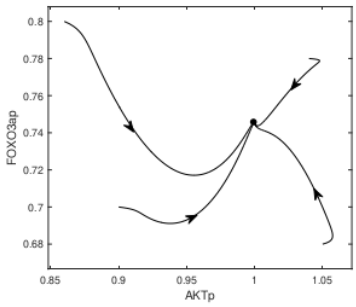

(c)

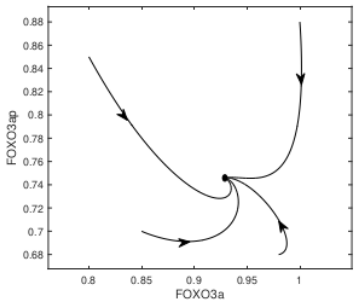

(d)

Fig. 3. The phase portrait projection confirms that the equilibrium point $E_{11}^{*} = (0.49055, 0.03178, 1.0000, 0.92775, 0.74556)$ is locally asymptotically stable.

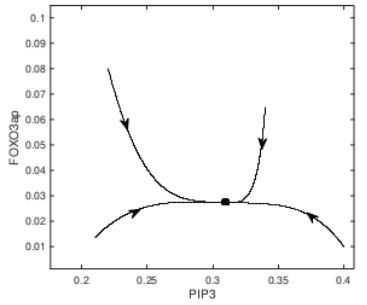

(a)

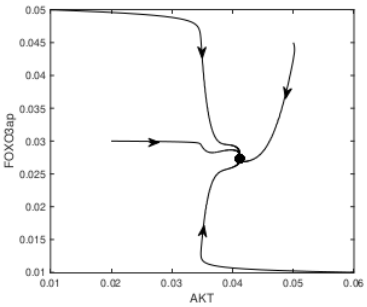

(b)

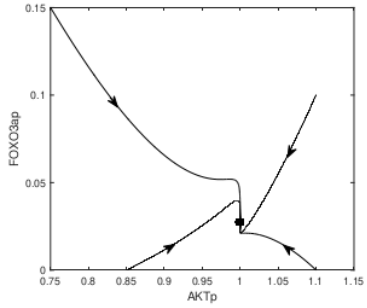

(c)

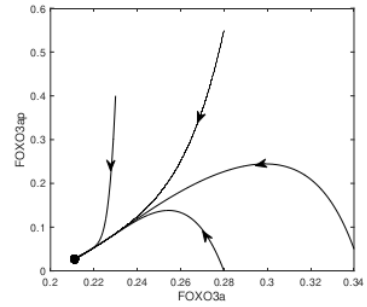

(d)

Fig. 4. The phase portrait projection confirms that the equilibrium point $E_{12}^* = (0.30991, 0.04122, 1.0000, 0.21113, 0.02735)$ is locally asymptotically stable.

from different initial values will tend to the equilibrium point, with FOXO3ap always tend to zero. It agrees with the Theorem 4.3 that, for a smaller production rate of FOXO3a p, the FOXO3ap can be eventually eliminated. In a medical point of view, these results suggest that the AML cell does not occur. This is consistent with the fact that FOXO3a does not present in the cytoplasm, indicated with zero concentration of FOXO3ap. Biologically, it means that cells are in normal condition and AML will not grow.

Fig.2 shows that the equilibrium point E_{11}^* is locally asymptotically stable. We can see that all trajectories which starting from different initial values will tend to the equilibrium point, with FOXO3ap always tend to a certain values. In a medical prespective, the AML cells occur and can be controlled. Fig.3 shows the local asymptotic stability of equilibrium point E_{11}^* and Fig.4 shows the local asymptotic stability of equilibrium point E_{12}^*. In Fig.3, it can be seen that if we choose an initial condition which is close enough to the equilibrium E_{11}^*, then the trajectory of the system is tend to E_{11}^*, whereas in Fig.4, if the initial condition is close enough to E_{12}^*, then the solution will tend to E_{12}^*. We can see that all trajectories tend to these equilibria provided that the initial conditions are sufficiently close to these equilibria. We note that E_{11}^* has higher FOXO3a and FOXO3ap concentration, while E_{12}^* has lower FOXO3a and FOXO3ap concentration. Therefore, in this case, the system has two stable equilibria and one unstable equilibrium point. It is observed that the equilibrium point with lower FOXO3a and FOXO3ap concentrations E_{12}^* is very close to the AML-free equilibrium point E_0 as in case (i). So in this case, we do hope that the equilibrium point tends to the lower FOXO3ap concentration E_{12}^* rather than the higher FOXO3ap concentration E_{11}^*. Medically, with condition of lower FOXO3ap concentrations, it is easier to treat AML than a higher concentration condition.

We also give an illustration that the region of attraction of the two stable equilibria is separated by the dashed trajectory in the phase plane diagram (see Fig. 5). As shown in Fig. 5, the unstable equilibrium point separating the basin of attractions of the two stable equilibria. Medically, if the trajectories convergen to the equilibrium point E_{1i}^*, then the AML cell will persist in the patient.

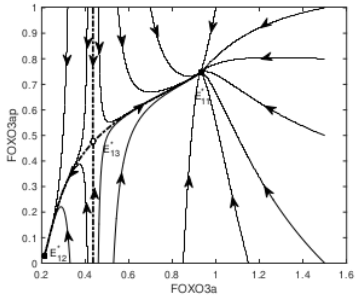

Fig. 5. Phase plane diagram showing the two stable equilibria for $p = 0.36$.

In order to determine AML treatment, we have to find the analytical conditions so that the trajectories of the system converges to the AML-free equilibrium point E_0.

This analytical condition is given in Theorem 4.3, that is the equilibrium point E_0 of the system (1) is locally asymptotically stable if $\Gamma < 1$. So, we can then choose varies values for the parameters p, m, a_2, k_4, or K_4, and observe the changes that occur in system behavior. In the next section, we provide a sensitivity analysis to identify how changes in each of these parameters affect system behavior.

VI. Sensitivity Analysis

In this section, the sensitivity indices of Γ will be analyzed. The sensitivity analysis can be used to discover a key parameters that have a high impact on the transmission and spread of AML disease and should be intervened by targeted therapy. We calculate the sensitivity index which is defined as the ratio of the relative change in Γ to the relative change in a parameter p, as follows [26], [27]:

$$\Upsilon_s^{\Gamma} = \frac{\partial \Gamma}{\partial s} \times \frac{s}{\Gamma}. \tag{17}$$

Now, we can derive the sensitivity indices of Γ from the explicit formula (13) by using (17) for each of the six different parameters described in Table I. The sensitivity index of Γ may depend on several parameters, but also can be constant, does not depend on any parameter values. For example, the sensitivity index of Γ with respect to constant rate of FOXO3a production, p is $\Upsilon_p^{\Gamma} = \frac{\partial \Gamma}{\partial p} \times \frac{p}{\Gamma} = +1$, does not depend on any parameter values. It is meaning that increasing (decreasing) of p, say 10 %, leads to 10 % increasing (decreasing) of Γ. The values of the sensitivity indices for the parameter values of case (i) are presented in Table II. From Table II, it can be seen that the sign of the sensitivity indices with respect to all parameters (i.e., whether Γ increases or decreases when a parameter increases) agrees with an intuitive expectation. For example, since $\Upsilon_{k_4}^{\Gamma} = -0.7605$ then increasing (or decreasing) the phosphorylation rate of FOXO3a by 10 % decreases (or increases) Γ by 7.605%. As illustration, in case (i), if we increase k_4 from 0.04 to 0.044 then Γ decrease from 0.8555 to 0.795.

TABLE II
The Sensitivity Indices of Γ

Parameter	Sensitivity index
p	$+1$
m	-0.2395
k_4	-0.7605
d_3	$+0.7605$
a_2	-0.7605
K_4	$+0.2535$

According to Table II, the most sensitive parameter is p, i.e the production rate of FOXO3a, so we should pay special attention to this parameter. Note that in case (i), with the parameter value of $p = 0.2$, we have $\Gamma = 0.8555$. In order to keep the stability of AML-free equilibrium point E_0, the threshold value Γ must less than one. Because the sensitivity index of Γ with respect to the constant rate of FOXO3a production p is $\Upsilon_p^{\Gamma} = +1$, it can be seen that if p increases by 14.45 % from 0.2 to 0.23377 result to the value of $\Gamma = 1$, so that the AML-free equilibrium point E_0 failed to have stability. So p must be kept to less than 0.23377.

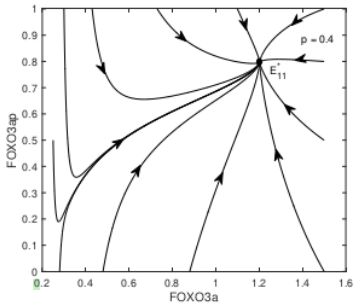

(a)

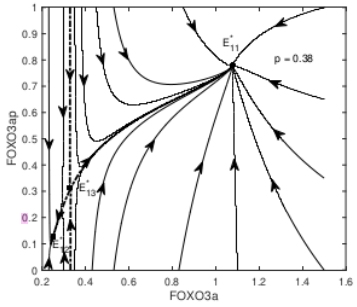

(b)

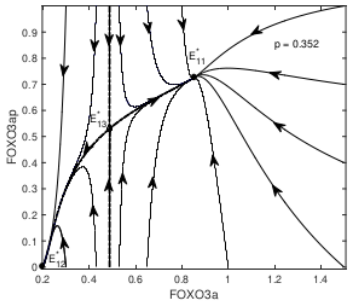

(c)

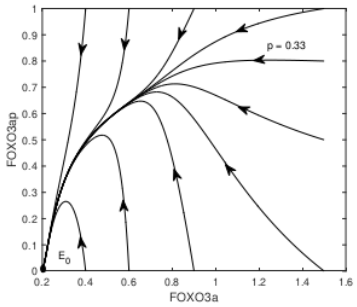

(d)

Fig. 6. The phase plane diagram for various values of p.

Medically, controlling the production rate of FOXO3a is an alternative way that can be done to improve the success of AML treatment. Thus, the production rate of FOXO3a should be targeted by intervention strategies.

Furthermore, by using the set of parameter values in case (ii), we can see the changes in a system behavior if the value of the parameter p is changed in Fig.6. In Fig.6a, if we set the values of $p = 0.4$, the system (1) only have one stable equilibrium point with high FOXO3ap concentration E_{11}^*. For smaller values of p, a separatrix appears which reduces the basin of attraction of E_{11}^*. As seen in Fig.6b, if we set the value of $p = 0.38$, there are two stable equilibria, E_{11}^* and E_{12}^* and one saddle point E_{13}^*. For $p = 0.352$, then the separatrix shift to the right reduces the basin of attraction of equilibrium point with a high concentration of FOXO3ap E_{11}^*, and enlarges the basin of attraction of E_{12}^*, see Fig.6c.

Furthermore, if the values of p reduced to $p = 0.33$, then the system (1) only have one AML-free equilibrium point E_0 and the system changes from bistable to monostable, see Fig.6d. The qualitative behavior for various parameter p can be summarized on a bifurcation diagram as shown in Fig.7.

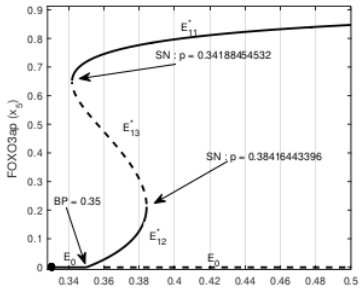

Fig. 7. A schematic of a bifurcation diagram showing bistable behavior for system (1)with various values of p. The solid curves depict stable behavior and the dashed curves depict unstable behavior.

The bifurcation diagram in Fig.7 shows that the system (1) only have one stable equilibrium point E_{11}^* whenever $p > 0.38416443396$. In this case, there is transcritical bifurcation at $p = 0.35$ and saddle-node bifurcations at $p = 0.38416443396$ and $p = 0.34188454532$, respectively. Bistable behavior exist whenever $0.34188454532 < p < 0.38416443396$.

VII. Conclusion

In this paper, we investigate the PI3K/AKT pathway in AML with biochemical reactions following the Hill's equation. We consider that the dephosphorylation of protein does not work properly. This is due to the fact that in AML there is a deletion or decrease in phosphatase levels. Furthermore, we show the existence of equilibria and established conditions for the stability of these equilibria.

For the condition of Theorem 4.3, we can say that if the production rate of FOXO3a is restricted the degradation and phosphorylation term of FOXO3a, then the AML-free equilibrium point E_0 is locally asymptotically stable. If the opposite condition occurs, the AML-free equilibrium point E_0 loses stability, and the equilibrium point E_{1i}^*, $i = 1, 2, 3, 4$ may occur. Unlike the AML-free equilibrium point E_0, for the equilibrium point E_{1i}^*, $i = 1, 2, 3, 4$ we cannot find the mathematical formula that can be used as a measure such that AML disease can heal or continue. Theorem 4.4 only provide the necessary condition so that the equilibrium point E_{1i}^*, $i = 1, 2, 3, 4$ become locally asymptotically stable.

We note that in the analysis of this model, it is assumed that there is a deletion of phosphatase which causes protein dephosphorylation does not occur. As a result, phosphorylated proteins cannot return to an unphosphorylated state. As can be seen from numerical simulations, the concentration of AKTp in all cases is always at the same amount of concentration, which is equal to the ratio of AKT production and AKTp degradation. This is due to the absence of AKT degradation and AKTp dephosphorylation. Different conditions will occur if there is protein dephosphorylation. Such conditions also occur in FOXO3a. We found that, without dephosphorylation of FOX3ap, when FOXO3a undergoes translocation from the nucleus to the cytoplasm through phosphorylation, FOXO3a cannot return to the nucleus. Furthermore, FOXO3ap in the cytoplasm will increase the continuity of the PI3K/AKT pathway. From the model, it was found that the greater the FOXO3a in the nucleus, the greater the translocation of FOXO3a to the cytoplasm. We have shown that if the rate of FOXO3a production is less than the total ammount of degradation and phosphorylation of FOXO3a, AML cells can be eliminated. Mathematically, this is indicated by the condition that the AML-free equilibrium point E_0 is locally asymptotically stable.

Finally, from the sensitivity analysis, we found that the most important parameter for AML disease is the production rate of FOXO3a. Thus, one way that can be done to reduce FOXO3ap in the cytoplasm is to inhibit the growth rate of FOXO3a. Medically, treatment of AML patients can be done through targeted therapy on the production of FOXO3a.

Acknowledgment

The authors would like to express their gratitude to the editors and anonymous reviewers for useful comments and suggestions. The special thanks also to the Cancer Modeling Team UGM for the discussions during the research.

References

[1] H. Dohner, E. Estey, and D. Grimwade, "Diagnosis and management of aml in adults: 2017 eln recommendations from an international expert panel," *Blood*, vol. 129, no. 4, pp. 424–447, 2017.

[2] L. Herschbein and J. L. Liesveld, "Dueling for dual inhibitor: Means to enhance effectiveness of pi3k/akt/mtor inhibitors in aml," *Blood Rev.*, vol. 32, no. 3, pp. 235–248, 2018.

[3] G. A. Horne, R. Kinstrie, and M. Copland, "Novel drug therapies in myeloid leukemia," *Pharm. Pat. Anal.*, vol. 4, no. 3, pp. 187–205, 2015.

[4] Y. Shen, J. Bai, and A. He, "Role of mtor signaling pathway in acute myeloid leukemia," *Int J Clin Exp Med*, vol. 9, no. 2, pp. 637–647, 2016.

[5] B. Beagle and D. A. Fruman, "The pi3k-akt-mtor signaling network in aml," in *Targeted Therapy of Acute Myeloid Luekemia*, M. Andreeff, Ed. USA: Springer, 2015, pp. 335–362.

[6] M. Farhan, H. Wang, U. Gaur, P. Little, J. P. Xu, and W. Zheng, "Foxo signaling pathways as therapeutic targets in cancer," *Int. J. Biol. Sci*, vol. 13, no. 7, pp. 815–827, 2017.

[7] S. M. Kornblau, N. Singh, Y. Qiu, W. Chen, N. Zhang, and K. R. Coombes, "Highly phosphorylated foxo3a is an adverse prognostic factor in acute myeloid leukemia," *Clin. Cancer Res.*, vol. 16, no. 6, pp. 1865–1874, 2010.

[8] R. S. Nho and P. Hergert, "Foxo3a and disease progression," *World J. Biol. Chem*, vol. 5, no. 3, pp. 346–354, 2014.
[9] C. M. Santamaria, M. C. Chillon, R. Garcia-Sanz, C. Perez, M. D. Caballero, F. Ramos, and et al, "High foxo3a expression is associated with a poor prognosis in aml with normal cytogenetics," *Leuk. Res*, vol. 33, no. 12, pp. 1706–1709, 2009.
[10] R. Polak and M. Buitenhuis, "The pi3k/pkb signaling module as key regulator of hematopoiesis: implications for therapeutic strategies in leukemia," *Blood*, vol. 119, no. 4, pp. 911–923, 2012.
[11] G. D. Clapp and D. Levy, "A review of mathematical models for leukemia and lymphoma," *Drug Discovery Today Disease Models*, vol. 16, pp. 1–6, 2015.
[12] A. Besse, G. D. Clapp, S. Bernard, F. E. Nicolini, D. Levy, and T. Lepoutre, "Stability analysis of a model of interaction between the immune system and cancer cells in chronic myelogenous leukemia," *Bull. Math. Biol*, vol. 80, no. 5, pp. 1084–1110, 2018.
[13] Y. Arkun, "Dynamic modeling and analysis of the crosstalk between insulin/akt and mapk/erk signaling patways," *PloS ONE*, vol. 110, no. 3, pp. 1–3, 2016.
[14] M. Behar, D. Barken, S. L. Werner, and A. Hoffmann, "The dynamics of signaling as a pharmacological target," *Celll*, vol. 155, no. 2, 2013.
[15] F. Pappalardo, G. Russo, S. C. S, M. Pennisi, S. Cavalieri, S. Motta, and et al, "Computational modeling of pi3k/akt and mapk signaling pathways in melanoma cancer," *PloS ONE*, vol. 11, no. 3, 2016.
[16] G. Wang, *Analysis of Complex Diseases*. Taylor & Francis Group: CRC Press, 2014.
[17] Y. A. Adi, F. Adi-Kusumo, L. Aryati, and M. S. Hardianti, "A dynamic model of pi3k/akt pathways in acute myeloid leukemia," *Journal of Applied Mathematics*, 2018.
[18] T. M. Kadia, F. Ravandi, J. Cortes, and H. Kantarjian, "New drugs in acute myeloid leukemia," *Annals of Oncology*, vol. 27, pp. 770 – 778, 2016.
[19] G. J. Schiller, P. Tuttle, and P. Desai, "Allogeneic hematopoietic stem cell transplantation in flt3-itd-positive acute myelogenous leukemia: The role for flt3 tyrosine kinase inhibitors post-transplantation," *Biol. Blood Marrow Transplant*, vol. 22, no. 6, pp. 982 – 990, 2016.
[20] B. P. Ingalls, *Mathematical Modelling in Systems Biology: An Introduction*. MIT Press, 2013.
[21] M. Santillan, "On the use of the hill functions in mathematical models of gene regulatory network," *Math. Model. Nat. Phenom*, vol. 3, no. 2, pp. 85 – 97, 2008.
[22] T. Pu, X. P. Zhang, F. Liu, and W. Wang, "Coordination of the nuclear and cytoplasmic activities of p53 in response to dna damage," *Biophysical Journal*, vol. 99, pp. 1696–1705, 2010.
[23] H. K. Khalil, *Nonlinear System*. Prentice-Hall, 2002.
[24] J. Yan-Bin, *Roots of Polynomial*, Com S 477/577 Notes, 2016.
[25] H. Miao and C. Kang, "Stability and hopf bifurcation analysis of an hiv infection model with saturation incidence and two time delays," *Engineering Letters*, vol. 27, no. 1, pp. 9 – 17, 2019.
[26] S. Olaniyi, M. A. Lawal, and O. S. Obabiyi, "Stability and sensitivity analysis of a deterministic epidemiological model with pseudo-recovery," *IAENG International Journal of Applied Mathematics*, vol. 46, no. 2, pp. 160 – 167, 2016.
[27] N. Chitnis, J. M. Hyman, and J. M. Cushing, "Determining important parameters in the spread of malaria through the sensitivity analisys of a mathematical model," *Bull. Math. Biol*, vol. 70, no. 5, pp. 1272 – 1296, 2008.

hasil-Analysis of a Mathematical Model of the Interaction between PIP3, AKT, and FOXO3a in Acute Myeloid Leukemia

ORIGINALITY REPORT

15%	9%	12%	4%
SIMILARITY INDEX	INTERNET SOURCES	PUBLICATIONS	STUDENT PAPERS

PRIMARY SOURCES

1	Y. A. Adi, A. Thobirin. "BACKWARD BIFURCATION IN A WITHIN-HOST TUBERCULOSIS MODEL", Advances in Mathematics: Scientific Journal, 2020 Publication	1%
2	Nakul Chitnis. "Determining Important Parameters in the Spread of Malaria Through the Sensitivity Analysis of a Mathematical Model", Bulletin of Mathematical Biology, 07/2008 Publication	1%
3	epdf.pub Internet Source	1%
4	www.iaeng.org Internet Source	1%
5	j.mecs-press.net Internet Source	1%
6	Submitted to Cranfield University Student Paper	<1%

7	Feng, Xiaomei, Shigui Ruan, Zhidong Teng, and Kai Wang. "Stability and backward bifurcation in a malaria transmission model with applications to the control of malaria in China", Mathematical Biosciences, 2015. Publication	<1 %
8	www.hindawi.com Internet Source	<1 %
9	I. R. Stella, Mini Ghosh. "Modeling plant disease with biological control of insect pests", Stochastic Analysis and Applications, 2019 Publication	<1 %
10	SOURAV KUMAR SASMAL, DIBYENDU SEKHAR MANDAL, JOYDEV CHATTOPADHYAY. "A PREDATOR-PEST MODEL WITH ALLEE EFFECT AND PEST CULLING AND ADDITIONAL FOOD PROVISION TO THE PREDATOR — APPLICATION TO PEST CONTROL", Journal of Biological Systems, 2017 Publication	<1 %
11	ebin.pub Internet Source	<1 %
12	Geoffrey Clapp, Doron Levy. "A review of mathematical models for leukemia and lymphoma", Drug Discovery Today: Disease Models, 2015 Publication	<1 %

13	Stephen Lynch. "Dynamical Systems with Applications Using Mathematica®", 'Springer Science and Business Media LLC', 2017 Internet Source	<1 %
14	www.cambridge.org Internet Source	<1 %
15	Submitted to ABV-Indian Institute of Information Technology and Management Gwalior Student Paper	<1 %
16	academic.oup.com Internet Source	<1 %
17	www.tandfonline.com Internet Source	<1 %
18	Avila-Vales, Eric, Noé Chan-Chí, and Gerardo García-Almeida. "Analysis of a viral infection model with immune impairment, intracellular delay and general non-linear incidence rate", Chaos Solitons & Fractals, 2014. Publication	<1 %
19	hdl.handle.net Internet Source	<1 %
20	public.lanl.gov Internet Source	<1 %
21	Lu, Yanling, and Guoping Jiang. "Backward bifurcation and local dynamics of epidemic	<1 %

model on adaptive networks with treatment", Neurocomputing, 2014.
Publication

22	Submitted to Middle East Technical University Student Paper	<1 %
23	Swarnali Sharma, G. P. Samanta. "Stability analysis and optimal control of an epidemic model with vaccination", International Journal of Biomathematics, 2015 Publication	<1 %
24	Yiling Liu, Qiegen Liu, Minghui Zhang, Qingxin Yang, Shanshan Wang, Dong Liang. "IFR-Net: Iterative Feature Refinement Network for Compressed Sensing MRI", IEEE Transactions on Computational Imaging, 2020 Publication	<1 %
25	Hui Miao, Chengjun Kang. "Stability and Hopf bifurcation analysis for an HIV infection model with Beddington–DeAngelis incidence and two delays", Journal of Applied Mathematics and Computing, 2018 Publication	<1 %
26	Meng, X.. "Profitless delays for a nonautonomous Lotka-Volterra predator-prey almost periodic system with dispersion", Applied Mathematics and Computation, 20070501 Publication	<1 %

27	Submitted to University of Stellenbosch, South Africa Student Paper	<1%
28	Tanvi, Rajiv Aggarwal. "Dynamics of HIV-TB co-infection with detection as optimal intervention strategy", International Journal of Non-Linear Mechanics, 2020 Publication	<1%
29	Apollos Besse, Geoffrey D. Clapp, Samuel Bernard, Franck E. Nicolini, Doron Levy, Thomas Lepoutre. "Stability Analysis of a Model of Interaction Between the Immune System and Cancer Cells in Chronic Myelogenous Leukemia", Bulletin of Mathematical Biology, 2017 Publication	<1%
30	HANNAH MICHALSKA and FAZAL-UR REHMAN. "Guiding functions and discontinuous control: the underwater vehicle example", International Journal of Control, 1/10/1998 Publication	<1%
31	Submitted to Swinburne University of Technology Student Paper	<1%
32	dspace.vsb.cz Internet Source	<1%

33	www.freepatentsonline.com Internet Source	<1 %
34	www.worldscientific.com Internet Source	<1 %
35	F. Belkhouche. "Trajectory-based optimal linearization for nonlinear autonomous vector fields", IEEE Transactions on Circuits and Systems I: Regular Papers, 2005 Publication	<1 %
36	Submitted to University of Venda Student Paper	<1 %
37	link.springer.com Internet Source	<1 %
38	window.edu.ru Internet Source	<1 %
39	Amy Turner, Chanok Jung, Pan Tan, Srinivas Gotika, Vijay Mago. "A comprehensive model of spread of malaria in humans and mosquitos", SoutheastCon 2015, 2015 Publication	<1 %
40	Shi Bai, F.M.A. Salam. "Disturbance-generated bifurcation in a prototype adaptive system with e/sub 1/-modification law", IEEE Transactions on Automatic Control, 1988 Publication	<1 %
	download.atlantis-press.com	

41	Internet Source	<1%
42	www.engineeringletters.com Internet Source	<1%
43	www.sec.gov Internet Source	<1%
44	J. Přívratská. "Disorientation Angle Expressed in Terms of Lattice Parameters", Ferroelectrics, 6/1/2003 Publication	<1%
45	Manoj Kumar Singh, B. S. Bhadauria. "Qualitative Analysis of an Additional Food Provided Predator–Prey Model in the Presence of Allee Effect", International Journal of Applied and Computational Mathematics, 2017 Publication	<1%
46	Stephen M. Sykes, Steven W. Lane, Lars Bullinger, Demetrios Kalaitzidis et al. "AKT/FOXO Signaling Enforces Reversible Differentiation Blockade in Myeloid Leukemias", Cell, 2011 Publication	<1%
47	d-nb.info Internet Source	<1%

48	ANN N. Mwambia, Mark O. Okongo, Gladys G. Njoroge. "Stability analysis of a mathematical model for awareness initiatives on registration of persons in Kenya", International Journal of Applied Mathematical Research, 2020 Publication	<1 %
49	Bassidy Dembele. "Malaria model with periodic mosquito birth and death rates", Journal of Biological Dynamics, 2009 Publication	<1 %
50	Jai Prakash Tripathi, Debaldev Jana, Vandana Tiwari. "A Beddington–DeAngelis type one-predator two-prey competitive system with help", Nonlinear Dynamics, 2018 Publication	<1 %
51	Muhammad Ozair, Abid Ali Lashari, Il Hyo Jung, Kazeem Oare Okosun. "Stability Analysis and Optimal Control of a Vector-Borne Disease with Nonlinear Incidence", Discrete Dynamics in Nature and Society, 2012 Publication	<1 %
52	Multidiscipline Modeling in Materials and Structures, Volume 6, Issue 4 (2013-05-27) Publication	<1 %
53	Nan Liu, Hongli Yang, Liangui Yang. "Dual roles of SIRT1 in the BAX switch through the	<1 %

	P53 module: A mathematical modeling study", Computational and Structural Biotechnology Journal, 2021 Publication	
54	Submitted to University of Northumbria at Newcastle Student Paper	<1 %
55	coek.info Internet Source	<1 %
56	hal.archives-ouvertes.fr Internet Source	<1 %
57	nar.oxfordjournals.org Internet Source	<1 %
58	nmbu.brage.unit.no Internet Source	<1 %
59	pdffox.com Internet Source	<1 %
60	powcoder.com Internet Source	<1 %
61	qdoc.tips Internet Source	<1 %
62	sinta3.ristekdikti.go.id Internet Source	<1 %
63	www.aimspress.com Internet Source	<1 %

64	www.degruyter.com Internet Source	<1%
65	www.ncbi.nlm.nih.gov Internet Source	<1%
66	www.sciencedirect.com Internet Source	<1%

Exclude quotes	On	Exclude matches	Off
Exclude bibliography	On		